Available online at www.sciencedirect.com
ScienceDirect
International Journal of Heat and Mass Transfer 50 (2007) 667–679
International Journal of HEAT and MASS TRANSFER
www.elsevier.com/locate/ijhmt

Natural convection heat transfer in horizontal and vertical closed narrow enclosures with heated rectangular finned base plate

S.A. Nada *

Mechanical Engineering Department, Benha High Institute of Technology, Benha 13512, Egypt

Received 13 January 2006; received in revised form 28 June 2006
Available online 27 September 2006

Abstract

Natural convection heat transfer and fluid flow characteristics in horizontal and vertical narrow enclosures with heated rectangular finned base plate have been experimentally investigated at a wide range of Rayleigh number (Ra) for different fin spacings and fin lengths. Quantitative comparisons of finned surface effectiveness (ε) and heat transfer rate between horizontal and vertical enclosures have been reported. In comparison with enclosure of a bare base plate, insertion of heat conducting fins always enhances heat transfer rate. Optimization of fin-array geometry has been addressed. The results gave an optimum fin spacing at which Nusselt number (Nu_H) and finned surface effectiveness (ε) are maximum. It has been found that: (1) increasing fin length increases Nu_H and ε; (2) increasing Ra increases Nu_H for any fin-array geometries and (3) for any fin-array geometry and at $Ra > 10{,}000$, increasing Ra decreases ε while for fin-array geometries of large fin spacing and at $Ra < 10{,}000$, increasing Ra increases ε. Useful design guidelines have been suggested. Correlations of Nu_H have been developed for horizontal and vertical enclosures. Correlations predictions have been compared with previous data and good agreement was found.

Keywords: Heat transfer; Narrow enclosure; Rectangular fins array; Vertical and horizontal

1. Introduction

Natural convection heat transfer in a fluid layer confined in a closed enclosure with partitions like fins is encountered in a wide variety of engineering applications of passive cooling of electronic equipment such as compact power supplies, portable computers and telecommunications enclosures. In the design of electronic packages, there are strong incentives to mount as much electronic components as possible in a given enclosure. This leads to high power generation density and this may rise the temperature of the packages above the allowable limit. To overcome this problem the heat transfer rate from the packages must be maximized. The most common technique of maximizing heat transfer rate is by using finned surfaces. The enhancement ratio of heat transfer depends on the fins orientations and the geometric parameters of fins arrays. The most common configurations of using fins arrays in heat sinks involve horizontal or vertical surface plate to which fin arrays are attached.

Fluid flow and heat transfer characteristics in a fluid layer confined between two parallel plates maintained at different temperatures depend on plates orientation. In case of vertical plates, a fluid circulation consisting of rising stream on the heated wall and descending stream along the cold wall is formed. A vast amount of research has been devoted since 1970 to predict the total heat transfer rate between the plates [1–5]. In most of engineering applications, where equipment enclosure is partially divided by electronic components, the behavior of the enclosed fluid

* Tel.: +20 121723182; fax: +20 13 3230297.
E-mail address: samehnadar@yahoo.com

0017-9310/$ - see front matter © 2006 Elsevier Ltd. All rights reserved.
doi:10.1016/j.ijheatmasstransfer.2006.07.010

Nomenclature

A	heated base plate area of the enclosure
a	enclosure length
b	enclosure width (depth)
F_{ij}	view factor
G_i	irradiation
Gr	Grashof number
g	gravity acceleration
H	enclosure height
$\bar{h}$	average heat transfer coefficient
I	electric current
J	radiosity
k_a	thermal conductivity of air
k_g	thermal conductivity of Plexiglas
k_w	thermal conductivity of enclosure wall
L	fin length
Nu_H	Nusselt number based on $\bar{h}$
ΔNu_H	uncertainty in Nusselt number
Pr	Prandtl number
q	convection heat transfer rate from enclosure finned base plate
q_c	rate of heat losses by conduction from the enclosure walls
q_r	rate of heat transfer by radiation to the cold surface
Ra	Rayleigh number based on enclosure height
S	fin spacing
T	temperature
T_H	average surface temperature of hot base plate
T_C	average surface temperature of enclosure cold plate
t	fin thickness
t_w	enclosure wall thickness
V	voltage
α	thermal diffusivity
β	coefficient of volume expansion
ε	finned surface effectiveness
$\bar{\varepsilon}$	emissivity
σ	Stefan–Boltzman constant
υ	kinematic viscosity

departs from the behavior of a fluid enclosed between parallel plates. This forced many investigators to study heat transfer and fluid flow in partially divided enclosures [6–8].

By contrast in case of fluid layer confined between two horizontal parallel plates, the imposed temperature difference between the plates must exceed a finite value before the first signs of fluid motion and convective heat transfer are detected [9–13]. The Rayleigh number at this condition is known as critical Rayleigh number. Above the critical Rayleigh number, the flow consists of counterrotating two-dimensional cells rolling the cross-section. This flow pattern is known as Bénard cells. This cellular flow becomes considerably more complicated as Rayleigh number increases where the two-dimensional cells break up into three-dimensional cells. At even higher Rayleigh numbers the cells become narrower and the flow becomes oscillatory and turbulent [14–16]. Detailed surveys of these different flow regimes and various transitions in Bénard convection are widely available in the open literature [17–19].

On the other hand, over the past 40 years, numerous investigations have been carried out to study heat transfer and fluid flow characteristics in rectangular fins attached to horizontal and vertical surfaces in free environment [20–30]. In these studies, the effects of fins spacing, fin length, fin thickness, fin thermal conductivity and fins orientations on free convection heat transfer and fluid flow characteristics were experimentally or numerically investigated. Design Correlations and optimization of fin-array geometry for maximum heat transfer rate and fin effectiveness has been addressed by most of these studies.

As shown above, the available literature revealed that a large number of investigations concerning fluid flow and heat transfer characteristics in a fluid layer of closed enclosures and in rectangular fins attached to vertical and horizontal bases in free environment have been experimentally and theoretically conducted. However, investigations with arrays of rectangular fins attached to horizontal or vertical surfaces in confined spaces such as closed enclosures, as would be likely encountered in electronic cooling systems, are very limited. To the authors' knowledge, only two investigations in this filed were most recently conducted. Inada et al. [31] have carried out an experimental investigation to study the effects of vertical fins on heat transfer rate in a horizontal fluid layer in a finite extent. The heat transfer rates have been reported for a single value of fin height and for limited range of Rayleigh number and fin spacing. Arquis and Rady [32] conducted numerical experiments to investigate natural convection heat transfer and fluid flow characteristics from a horizontal fluid layer with finned bottom surface. The effects of fin height, fin spacing and Rayleigh number on fin surface effectiveness have been studied in a limited low range of Rayleigh number. To the best of our knowledge, there is no detailed experimental parametric study on heat transfer and fluid flow characteristics within a finned horizontal fluid layer. Also, study of heat transfer and fluid flow characteristics in a finned vertical fluid layer is not available in the literature. Investigations of the effects of the orientation of the fluid layer with finned surface, horizontal or vertical, on natural convection heat transfer are not available yet in the open literature. Therefore, the present work aims to present comprehensive experimental investigation to heat transfer and fluid flow characteristics in a horizontal and vertical fluid layers of narrow closed enclosures with rectangular finned base plate. For both

enclosures, horizontal and vertical, the effects of fin height and fin spacing have been investigated for a wide range of Rayleigh number. The results of this study are useful for geometric optimization and for developing practical design guidelines of passive cooling enhancement technique of closed enclosures using finned surfaces.

2. Experimental setup and procedure

2.1. Experimental setup

The experimental setup consists of a narrow enclosure of internal dimensions $a \times b \times H = 320 \times 200 \times 40$ mm. The enclosure height (H) is made small in comparison with the enclosure base dimensions (a and b) to make the air tends to circulate in a series of Bénard cells. Also, this reduces the effects of a and b on the results. The enclosure was mounted on a rotatable frame to vary the enclosure orientation from horizontal to vertical. The bottom and four side walls of the enclosure were made of double layers of 8-mm thick Plexiglass sheet with 5-cm thick fiberglass thermal insulation inserted between them. A 320×200 mm nickel–chrome wire panel heater (500 W) was used for heating the enclosure finned base plate. The heater consisted of a nickel-chrome wire wound round a thin mica plate and insulated from all sides with a mica sheet covered by a thin stainless steel sheet. The heater was internally mounted on the enclosure base. The finned base plate of the fin array was mounted on the enclosure heater. The top surface of the enclosure was closed by a water stainless steel box to maintain the enclosure top surface (the enclosure top surface is the bottom surface of the cooling water box) at constant low temperature (T_L) by circulating cooling water through the box at high flow rate. A cross-section view of the enclosure is shown in Fig. 1a.

The heater was connected with a DC power supply to control the power input. Voltage and current supplied to the heater were measured by digital voltmeter and ammeter of accuracy 0.025%. The surface temperature distribution of the base plate of the fin array was measured using 12 Teflon coated thermocouples (type K) equally spaced and distributed as shown in Fig. 1b. To facilitate thermocouples installation without disturbing free convection currents inside the enclosure, holes were drilled from the enclosure backside passing through enclosure double walls, heater and finned base plate. The thermocouples were inserted from these holes and their junctions were fixed on the top surface of the finned base plate as shown in Fig. 1a. To estimate conduction heat losses across enclosure walls, two thermocouples (type K) were fixed on the inner and outer surfaces (at the center) of each side wall of the enclosure. The temperature of enclosure cold top surface was measured by two thermocouples fixed on the bottom surface of the circulating water box as shown in Fig. 1a. The ambient temperature was measured by a separate thermocouple. All thermocouples were calibrated in a constant temperature path and a measurement accuracy of ± 0.2 °C was obtained. All temperature signals were acquired with a data acquisition system and sent into a PC for data recording.

Fig. 2 illustrates the fin-array geometry and dimensions of the finned base plate. The fins and base plate were made of copper. Enclosure internal dimensions and fins and base plate thickness ($t = 1.5$ mm) were kept constant in this work. The fins pitch S, number of fins and fin length L were the geometrical variables of the tested fin-arrays. Table 1 lists fins spacing, fins lengths and number of fins of all tested fin-arrays.

2.2. Experimental procedure

After mounting each fin-array in the enclosure, the input power was adjusted to give a certain Rayliegh number. Water is allowed to flow through the water box at high flow rate to maintain the top surface of the enclosure at low

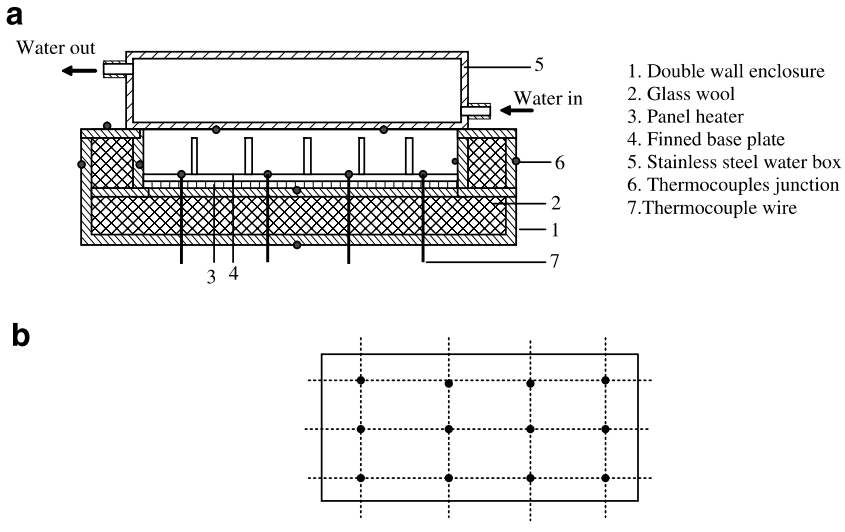

Fig. 1. Cross-section view of the enclosure and thermocouples locations: (a) cross-section view of the enclosure (horizontal orientation) and (b) thermocouples locations on base plate.

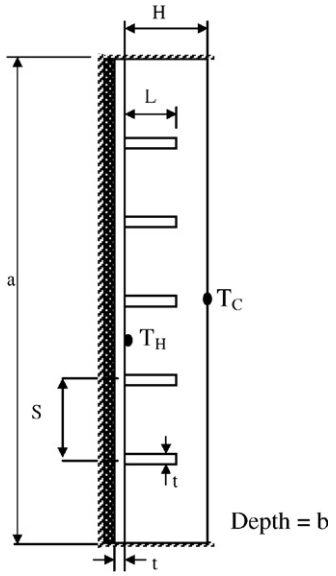

Fig. 2. Geometry of fin-array (vertical orientation).

Table 1
Fin-arrays configurations

Fin-array set	Fin length (L/H)	Fin spacing (S/H)	Fins number (N)
1	0.75	2	3
2	0.75	1.33	5
3	0.75	1	7
4	0.75	0.8	9
5	0.5	2	3
6	0.5	1.33	5
7	0.5	1	7
8	0.5	0.8	9
9	0.25	2	3
10	0.25	1.33	5
11	0.25	1	7
12	0.25	0.8	9
13 (Base case)	–	–	0 (No fins)

temperature. The experiment was allowed to run for at least 4 h until steady state condition was achieved. Steady state condition was considered to achieve when the differences in the measured base plate temperatures were not more than 0.2 °C over 30 min. After steady state condition has been established, readings of all thermocouples, input power and ambient temperature were recorded. For each fin-array geometry set listed in Table 1, about seven to eight experiments for different Rayleigh numbers varying from 5000 to 300,000 were carried out for each enclosure orientation; horizontal and vertical.

3. Data reduction

The dimensionless Rayleigh number (Ra) was calculated from the measured quantities as follows:

$$Ra = \frac{g\beta(T_H - T_C)H^3}{\alpha v} = GrPr \tag{1}$$

where T_H is the average temperature of the finned-base plate, T_C is the temperature of the enclosure top surface, H is enclosure height, g is the acceleration of gravity and β, v and α are the coefficient of volumetric expansion, kinematic viscosity, and thermal diffusivity of air, respectively. All air properties in Eq. (1) were taken at $(T_H + T_C)/2$. The energy balance for the enclosure gives

$$VI = q + q_c + q_r \tag{2}$$

where I and V are the electric current and voltage input to the heater, q is the heat transfer by free convection from the enclosure hot base plate to the enclosure cold plate through the fluid layer enclosed between them, q_C is the heat losses by conduction through enclosure walls and q_r is the heat transfer by radiation from enclosure internal sides and bottom walls to enclosure top surface. The conduction heat loss from the enclosure is the sum of the conduction heat losses through the walls of the enclosure surfaces except the cold surface. This is expressed as

$$q_c = \frac{1}{(2t_w/k_w + t_g/k_g)} \sum A_j \Delta T_j \tag{3}$$

where j is the wall identification number, k_w is the thermal conductivity of the Plexiglas, t_w is the thickness of the Plexiglas wall, k_g is the thermal conductivity of the fiberglass insulation inserted between the enclosure double walls, t_g is the thickness of the fiberglass insulation, A_j is the area of the j side wall of the enclosure, and ΔT_j is the temperature difference between the inner and outer surfaces of the j wall of the enclosure, respectively.

The radiation was incorporated in the losses based on the radiosity/irradiation formulation. All interior surfaces of the enclosure were assumed to be opaque, diffuse, isothermal and gray. The radiation heat loss q_r from the enclosure internal hot surfaces (sides and bottom surfaces) is the net rate at which radiation is incident on the cold surface of the enclosure. Identifying the enclosure internal hot surfaces by the number j, the net rate at which radiation is incident on the enclosure cold surface is calculated from

$$q_r = \bar{\varepsilon}_c A_c (\sigma T_c^4 - G_c) \tag{4}$$

where the irradiation G_c is given by

$$G_c = \sum_{j=1}^{5} F_{cj} J_j \tag{5}$$

where F_{cj} is the view factor between the enclosure cold surface and the jth surface of the enclosure and J_j is the radiosity of that surface and is given by

$$J_j = \bar{\varepsilon}_j \sigma T_j^4 + (1 - \bar{\varepsilon}_j) \sum_{i=1}^{5} F_{ji} J_i \tag{6}$$

The view factors F_{ij} between parallel and perpendicular surfaces were calculated based on the graphs and expressions given in Incropera and De Witt [33] and Suryanarayana [34]. Eqs. (4)–(6) were solved together to find the radiation heat losses in terms of the surfaces temperatures

of the enclosure inside walls. In all experiments, the conduction heat losses through the enclosure walls and the radiation heat transfer to the cold surface were within 4% and 5% of the input power, respectively.

The average heat transfer coefficient between the hot base plate and the cold plate of the enclosure is given by:

$$\bar{h} = \frac{q}{A(T_H - T_C)} \tag{7}$$

where A is the area of the base plate, T_H is the average temperature of the hot plate of the enclosure (taken as the average of the readings of the 12 thermocouples mounted on base plate) and T_C is the average temperature of the enclosure top surface (taken as the average of the readings of the two thermocouples fixed on this surface). The deviation between the readings of these two thermocouples was within 0.4 °C. The thermocouples readings are taken at a rate of 5 readings per second for a period of 60 s. The average of these 300 readings of each thermocouple was taken in the calculation of T_H and $\bar{h}$. The variations in theses 300 readings of all thermocouples were within 0.4 °C, even for large values of Ra. These steady readings of thermocouples indicate that the flow in the cavity is stable. This stability is returned to the small cavity height H (narrow cavity). Moreover, using fins inside the cavity makes the flow more stable due to viscous effects from the presence of the fins surfaces. Also, the high thermal conductivity of the base plate contributes in these steady readings of thermocouples. A numerical work is required to investigate the stability of the flow in narrow cavities with finned surfaces at high Ra where it is very difficult to experimentally address this phenomenon. Temperature measurements showed that the variation of the surface temperature distribution of the hot base plate was within 1 °C. This achieved uniform surface temperature is attributed to the high thermal conductivity of the base plate. The effects of the different parameters (S/H, L/H, and Ra) on flow behavior and heat transfer in the cavity is reflected as an increase or decrease in T_H.

The Nusselt number based on $\bar{h}$ is calculated from

$$Nu_H = \frac{\bar{h}H}{k_a} \tag{8}$$

where k_a is the thermal conductivity of the air taken at $(T_H + T_C)/2$. Combining Eqs. (2)–(8) together, the expression of $\overline{Nu}$ can be put on the form

$$Nu_H = f(x_1, x_2, \ldots\ldots x_n) \tag{9}$$

where x_1 to x_n are the variables that affect the experimental determination of $\overline{Nu}$. The uncertainty ΔNu_H in the value of Nu_H was estimated based on the procedure of Holman and Gajda [35] and is expressed as follows

$$\Delta Nu_H = \sqrt{\sum_{i=1}^{n} \left(\frac{\partial Nu_H}{\partial x_i} \Delta x_i \right)^2} \tag{10}$$

where Δx_i is the uncertainty in the x_i variable. The uncertainty in the various variables used in the determination of the Nusselt number were: 0.25% for the electric current I, 0.25% for the electric volt V, 0.2 °C for any temperature measurement, 0.001 m for any distance value, 0.5% for the thermal conductivity of air, 2% for the thermal conductivities of plexiglass and glass wool, and 5% for the emittance of the base plate and the plexiglass. It was found that the uncertainty for all data of Nu_H ranges from 4% to 9%.

4. Results and discussion

The experimental work was performed to study the effects of fin-array geometry (namely fin spacing and fin length), Rayleigh number and enclosure orientation (horizontal and vertical) on the heat transfer rate by free convection from the enclosure rectangular finned base plate to its top surface. Figs. 3–7 show the variation of the average Nusselt number with Rayleigh number at various fin spacing and fin length for horizontal and vertical enclosures.

4.1. Effect of fin spacing

The dependence of the Nusselt number (Nu_H) on fin spacing (S/H) for different values of fin lengths (L/H) and at the entire range of Rayleigh number (Ra) is shown in Figs. 3 and 4 for horizontal and vertical enclosures, respectively. Also, the variation of Nu_H with Ra for the basic case: base plate without fins is superimposed on these curves. Figs. 3 and 4 show that, for all fin-arrays and at any Rayleigh number, Nu_H of vertical and horizontal enclosures with finned heated base plates are higher than those of the base case without fins. Also Figs. 3 and 4 show that, for both vertical and horizontal enclosures, Nu_H increases with decreasing fin spacing (S/H) (i.e., with increasing number of fins) until it reaches a maximum at a certain (S/H). With further decreasing of fin spacing, Nu_H starts to decrease. The conditions at which Nu_H is maximum is important for optimum performance of fin-arrays in practical applications. Figs. 3 and 4 show that the value of S/H at which Nu_H is maximum independs on fin L/H and Ra. As shown in the figures, the maximum Nu_H occurs at $S/H = 1$ (number of fins = 7) for both horizontal and vertical enclosures. This variation of Nu_H with S/H can be attributed to the dependence of the heat transfer rate in the enclosed air layer upon the competition between the effects of the following factors on the heat transfer rate: (1) the increase of heat transfer surface area due to fins insertion, (2) the reduction or increase of the number of convection cells in the fluid layer with the insertion of more fins, and (3) the increase or decrease of the flow intensity with fins insertion. For both horizontal and vertical enclosures, as the number of fins increases the heat transfer surface area increases, and this tends to increase the rate of heat transfer. The flow field characteristics of horizontal and vertical fluid layers enclosed in a horizontal and

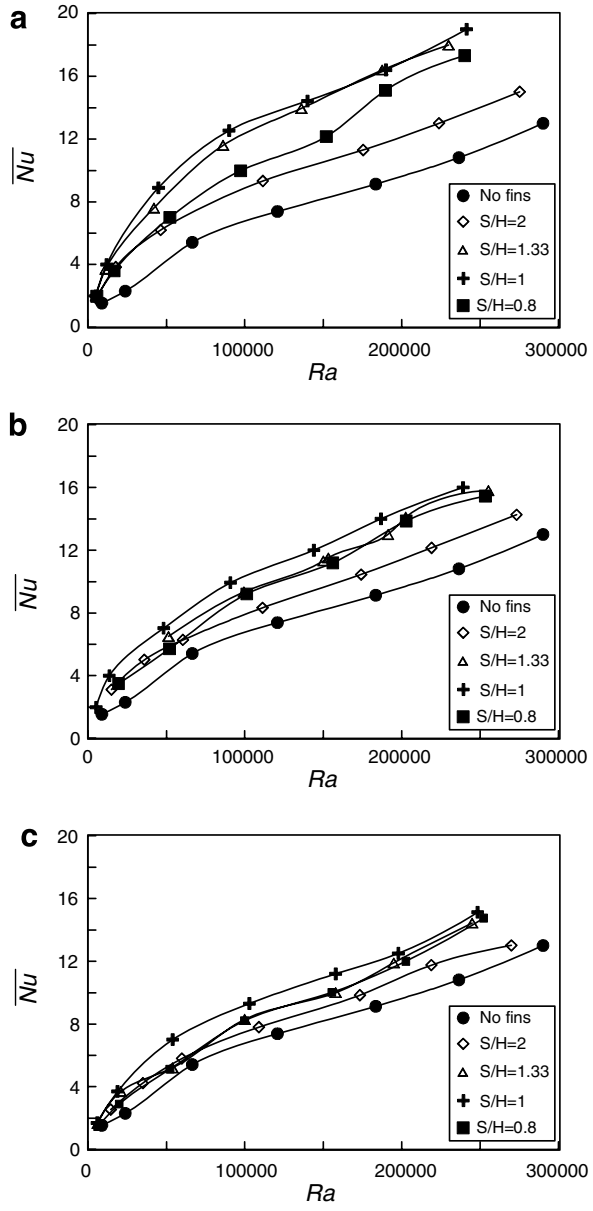

Fig. 3. Effect of fin spacing on Nusselt number for different fin lengths (horizontal enclosure): (a) $L/H = 0.75$; (b) $L/H = 0.5$ and (c) $L/H = 0.25$.

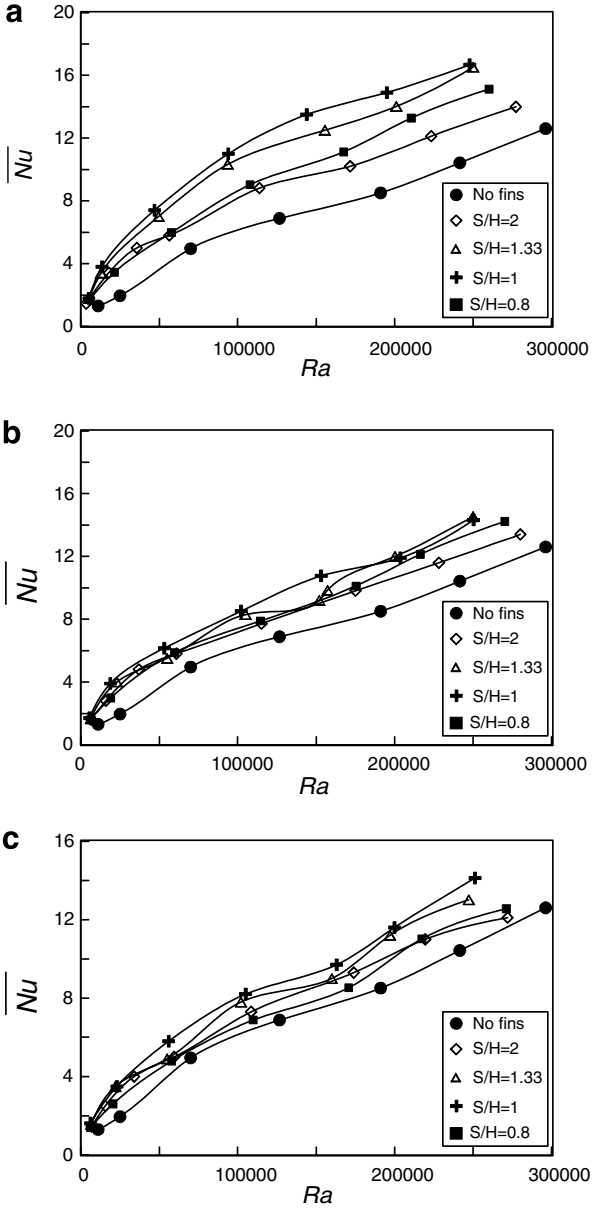

Fig. 4. Effect of fin spacing on Nusselt number for different fin lengths (vertical enclosure): (a) $L/H = 0.75$; (b) $L/H = 0.5$ and (c) $L/H = 0.25$.

vertical narrow enclosure is different as shown in Fig. 8. This flow filed characteristics was sketched based on the flow circulation given in the experimental work of [31], the numerical results of [32] and in other studies currently available in the literature [5,33,34] for finned and unfinned narrow enclosures. For a horizontal fluid layer without fins, the flow consists of counterrotating convection cells having almost square cross-section as shown in Fig. 8a(1). With fin insertion, Inada et al. [31] experimentally observed that the number of rotating convection cells increased as the number of fins increased from 3 to 7. Also, Arquis and Rady [32] numerically noticed the increase of the number of convection cells with the decrease of fin spacing for $Ra > 5000$. They also noticed the independence of the number of rotating convection cells on Ra and L/H at $Ra > 5000$. Therefore, previous numerical and experimental studies [31,32] showed that for $Ra > 5000$, increasing the number of fins (decreasing S/H) tends to increase the number of rotating convection cells as shown in Fig. 8a(2). Increasing the number of rotating convection cells leads to higher heat transfer rates. The resistance of the motion of the rotating convection cells is expected to increase with decreasing S/H and this leads to weaker flow intensity. Decreasing flow intensity reduces heat transfer rate. Based on this discussion, Fig. 3 provides that for $S/H > 1$, the increase of heat transfer as a result of increasing heat transfer surface area and as a result of increasing the number of convection cells overcomes the decrease of the heat transfer rate as a result of the decrease of flow intensity. The opposite is true for $S/H < 1$. The indepen-

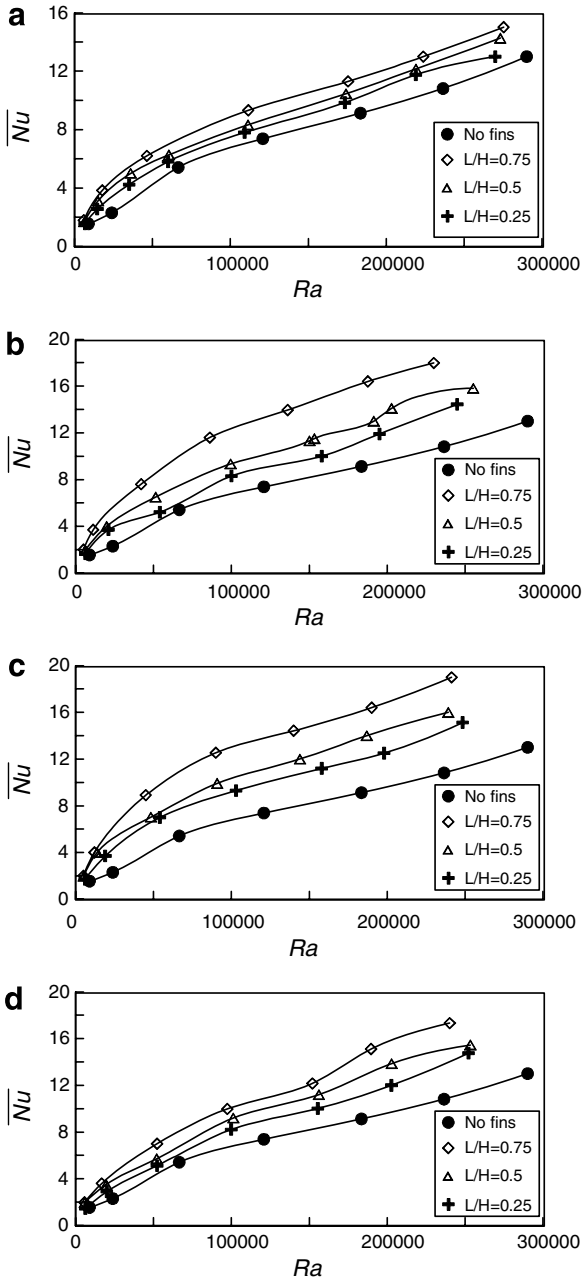

Fig. 5. Effect of fin length on Nusselt number for different fins spacings (horizontal enclosure): (a) $S/H = 2$; (b) $S/H = 1.33$; (c) $L/H = 1$ and (d) $S/H = 0.8$.

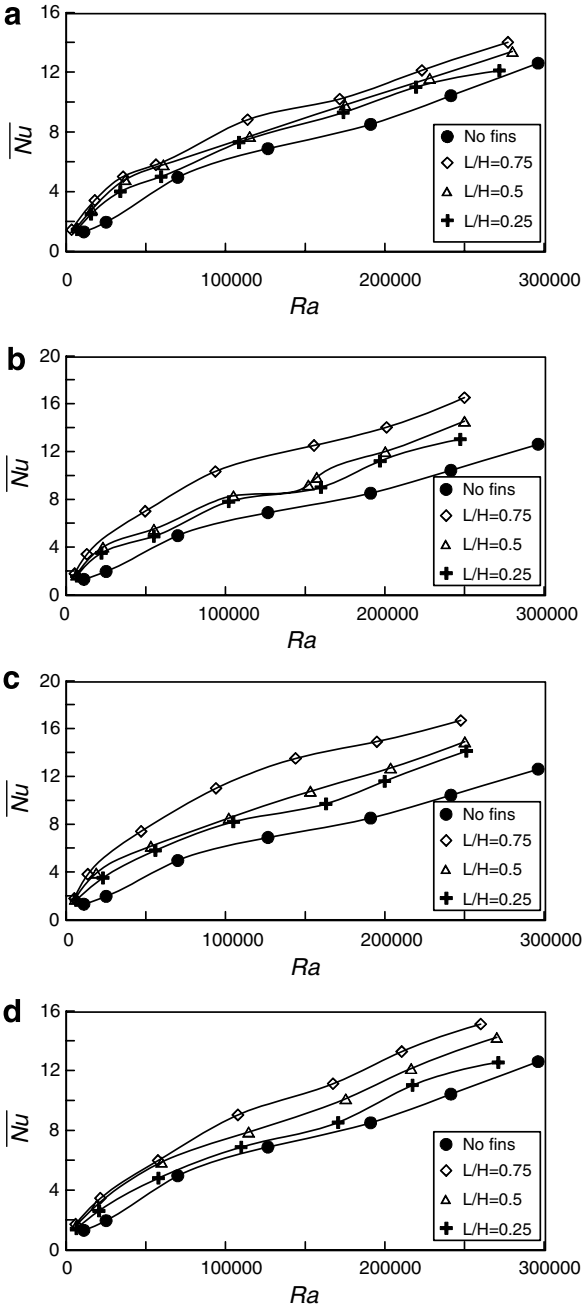

Fig. 6. Effect of fin length on Nusselt number for different fins spacings (vertical enclosure): (a) $S/H = 2$; (b) $S/H = 1.33$; (c) S/$H = 1$ and (d) $S/H = 0.8$.

dence of the value of S/H at which Nu_H is maximum on Ra and L/H can be attributed to the independence of the number of the rotating convection cells on Ra and L/H for the present range of Ra.

For a vertical fluid layer without fins, the flow field is characterized by a single circulation cell that rises along the heated wall and descends along the cold wall as shown in Fig. 8b(1). With fins insertion, the flow field depends on S/H and L/H as shown in Fig. 8b(2–4). For short fin lengths (see Fig. 8b(2)), the flow field is expected to be characterized by a single circulation cell with distortion of its shape at its contact surface with fins tips. Also for high fins density (low S/H), the fin spacing is too thin to permit the formation of convection cells between each adjacent two fins. A single convection cell is formed in the space between the fins tips and the cold wall with stagnant layers trapped between each adjacent fins as shown in Fig. 8b(3). At tall fins and large S/H, a separate rotating convection cell is expected to form between each two adjacent fins as shown in Fig. 8b(4). This effect of fins insertion on the flow filed provides that as the number of fins increases to a certain limit the number of convection cells increases and this tends to increase the rate of heat transfer. If the number

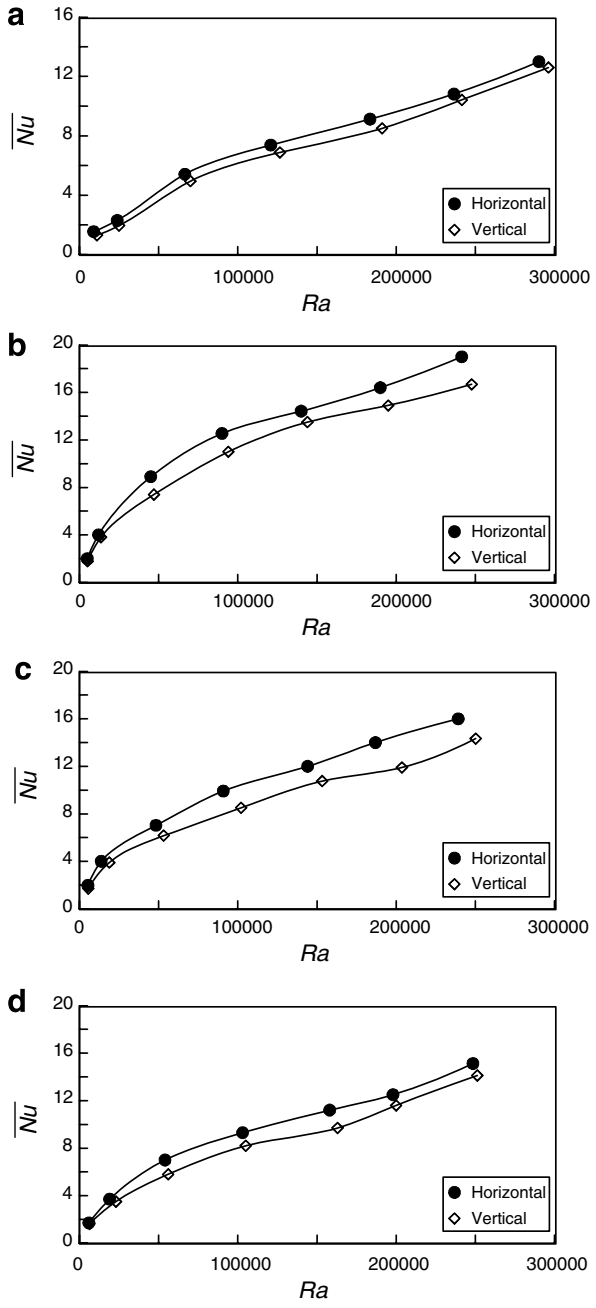

Fig. 7. Effect of enclosure orientation on Nusselt number for different fins spacings and fin lengths: (a) no fins; (b) $S/H = 1$ and $L/H = 0.75$; (c) $S/H = 1$ and $L/H = 0.5$ and (d) $S/H = 1$and $L/H = 0.25$.

of fins increased beyond this limit where fin spacing becomes too small to form a convection cell between fins, the heat transfer rate is dramatically decreases. Also, as for horizontal fluid layer, increasing the number of fins increases the resistance of the convection cells rotations and this tends to decrease the rate of heat transfer. Based on this discussion, Fig. 4 provides that for $S/H > 1$, the increase of heat transfer rate as a result of increasing heat transfer surface area and increasing the number of convection cells due to the increase of number of fins overcomes the decrease of the heat transfer rate as a result of the decrease of the flow intensity. For $S/H < 1$, the increase of the heat transfer as a result of increasing heat transfer surface area (due to the increase of number of fins) is not able to overcome the decrease of heat transfer rate due to the weakness of flow intensity and due to the inability of formation of convection cells between fins.

4.2. Effect of fin length

Figs. 5 and 6 show the effect of L/H on Nu_H for horizontal and vertical enclosures, respectively. Nu_H is plotted against Ra for different S/H with L/H as a parameter. As shown in Figs. 5 and 6, for both enclosure orientations and at any Ra and S/H, increasing L/H increases Nu_H. This can be attributed to the increase of heat transfer surface area with increasing L/H. Moreover, for a horizontal enclosure increasing L/H increases the possibility of dividing each convection cell into two cells as shown in Fig. 8a(3) and this leads to higher heat transfer rate. Also, for a vertical enclosure, increasing L/H increases the possibility of formation of a separate convection cell between each two adjacent fins (see Fig. 8b(4)) and this leads to higher heat transfer rates. However, for high fins density, where S/H is too small to form individual convection cells between fins, increasing L/H increases the resistance of convection cell movement and this slightly reduces heat transfer rate. This reduction of heat transfer rate cannot overcome the increase of heat transfer due to the increase of surface area and the net result was the increase of heat transfer with increasing L/H.

4.3. Effect of enclosure orientation

Fig. 7(a–d) shows the effect of enclosure orientation on Nu_H for bare base plate case and finned base plate case having $S/H = 1$ and $L/H = 0.75$, 0.5 and 0.25, respectively. The figure shows that the horizontal orientation of the enclosure has higher Nu_H than the vertical orientation. This trend was noticed for all S/H and L/H at the entire range of Ra. Thus, it can be concluded that fin-arrays orientation in closed enclosures is important for optimum performance of enclosures in practical applications. A narrow closed enclosure with a finned base plate is more preferable to be oriented with a horizontal finned base plate. The higher Nu_H of the horizontal orientation over the vertical orientation can be attributed to the expected higher number of rotating cells for the horizontal orientation than the vertical one.

4.4. Effect of Rayleigh number

Figs. 3–7 show the variation of Nu_H with Ra number for different S/H and L/H for horizontal and vertical enclosures. It can be observed from these figures that for any S/H and L/H and at both enclosure orientations, the average Nusselt number generally increases with increasing Ra. This can be attributed to the increase of the buoyancy force

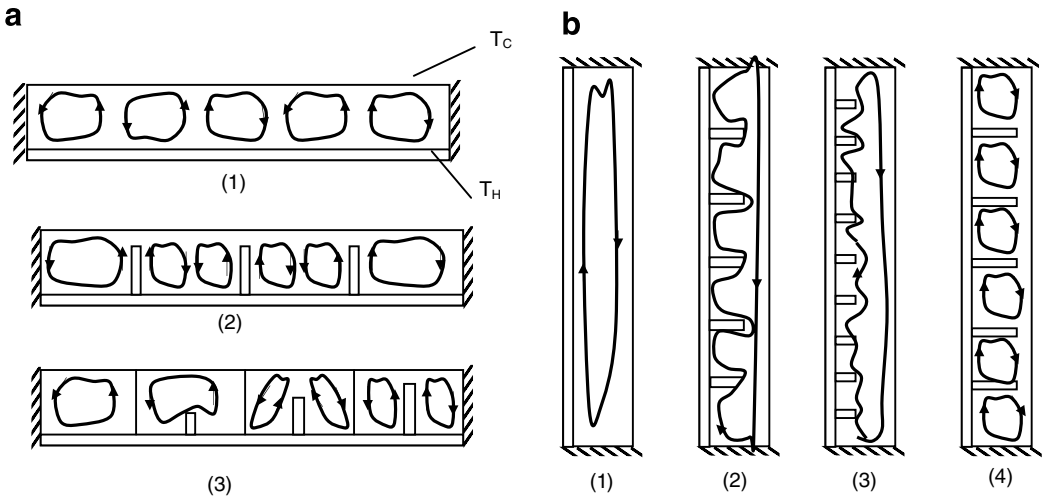

Fig. 8. Schematic of flow circulation inside the enclosure: (a) horizontal enclosure and (b) vertical enclosure.

with increasing Ra. Increasing buoyancy force increases flow driving force and in consequently causes an increase of flow intensity that leads to higher heat transfer rates. Also, increasing Ra enhances the mixing within the air layer due to the increase of turbulence of vortices that leads to better heat transfer performance.

5. Empirical correlations

Two different empirical correlations were developed from the experimental data to give the Nu_H in terms of Ra, S/H and L/H for horizontal and vertical enclosures, respectively. The characteristics and physics of heat transfer data, that was shown in Figs. 3–7, reveal that Nu_H increases with Ra and L/H according to a power function and varies with S/H according to a polynomial function. Therefore, the experimental data are fitted, using regression analysis, to give Nu_H as follows:

(a) For horizontal enclosure

$$Nu_H = 1.5Ra^{0.57}(L/H)^{0.25}(0.0215(S/H)^3 - 0.094(S/H)^2 + 0.127(S/H) - 0.042) \quad (11)$$

(b) For a vertical enclosure

$$Nu_H = 1.33Ra^{0.56}(L/H)^{0.22}(0.022(S/H)^3 - 0.096(S/H)^2 + 0.131(S/H) - 0.044) \quad (12)$$

These correlations are developed under the following ranges: $5000 \leqslant Ra \leqslant 300{,}000$, $0.25 \leqslant L/H \leqslant 0.75$ and $0.8 \leqslant S/H \leqslant 2$. To evaluate the predictions of these equations, the predictions of the equations are compared with the present experimental data in Figs. 9(a) and 9(b) at different values of Ra, S/L and H/L for horizontal and vertical enclosures, respectively. As shown in these figures, Eqs. (11) and (12) predict all the experimental data quite well. Fig. 9 shows that the deviation of the equations prediction from the experimental data is large at high values of S/H and Ra (see Figs. 9a(1) and 9b(1), whereas the deviation is large at $S/H = 2$ and $Ra > 150{,}000$). This can be attributed to that: at high values of S/H and Ra the stability of the flow in the cavity decreases due to the reduction in the viscous effects of the fins surfaces. The percentage of errors in the experimental data is expected to increases as the flow in the cavity becomes more unstable. Regression analysis using least square method showed that Eqs. (11) and (12) can predict all the experimental data with an error of $\pm 12\%$.

6. Comparison with literature

To the author's knowledge, no previous studies were carried out on natural convection heat transfer in vertical narrow enclosures with a heated finned base plate. Therefore, comparison of present data for a vertical enclosure cannot be conducted. For horizontal enclosures with a finned horizontal base plate, the present literature review revealed that only two papers are available in the literature, one is experimental [31] and the other is numerical [32]. These studies were carried out for a limited range of Ra ($2000 < Ra < 30{,}000$). To compare the results of the present study with the results of [31,32], Eq. (11) is used to predict Nu_H for Ra, S/H and L/H values which were used in these works. The results of the prediction are compared with their results in Fig. 10. Fig. 10 shows that Eq. (11) overpredicts the results of Inada et al. [31] by 24% for $S/H = 1.4$, while it well predicts their results for $S/H = 2$. The overprediction at $S/H = 1.4$ can be attributed to the difference of the enclosure height of the present study ($H = 40$ mm) and that of Inada et al. [32] ($H = 20$ mm), and also due to the difference of H/b between the present study ($H/b = 0.2$) and that of Inada et al. [32] ($H/b = 0.16$). The small enclosure height decreases the intensity of fluid motion and circulation, specially for smaller values of S/H, and this leads to smaller heat transfer rate.

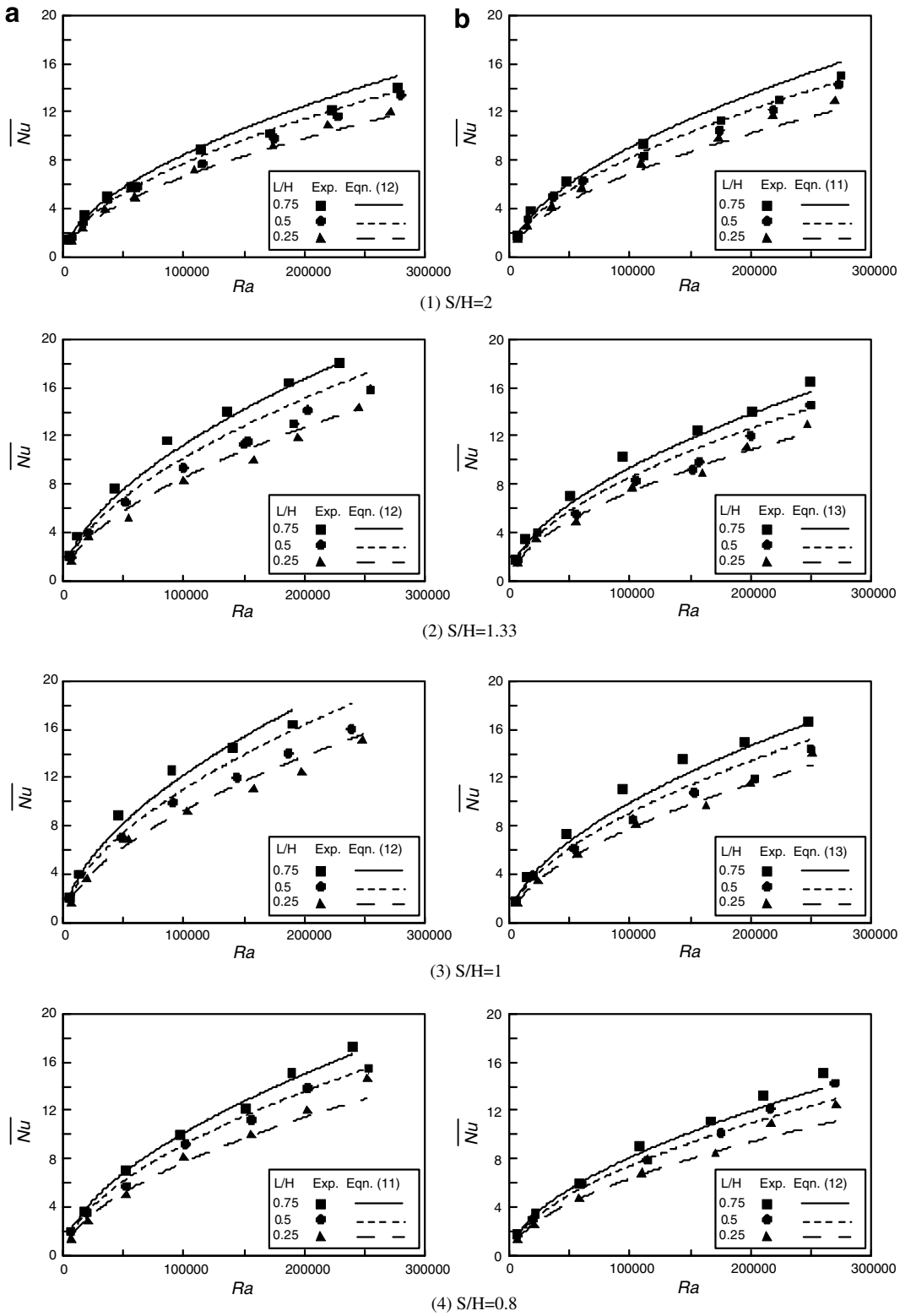

Fig. 9. Deviation of experimental data from the prediction of Eqs. (11) and (12): (a) horizontal enclosure and (b) vertical enclosure.

Also as H/b decreases, the number of convection cells decreases and this reduces heat transfer [32].

Fig. 10 shows that Nu_H of Arquis and Rady [32] is over the prediction of Eq. (11) by 25% at low Ra and this difference decreases with increasing Ra until it vanishes at $Ra \cong 30{,}000$. The differences between the present results and those of Arquis and Rady [32] can be attributed to their numerical simplifications of considering laminar incompressible flow and using a two-dimensional computational domain ignoring the 3-D effect. In natural convection cavity

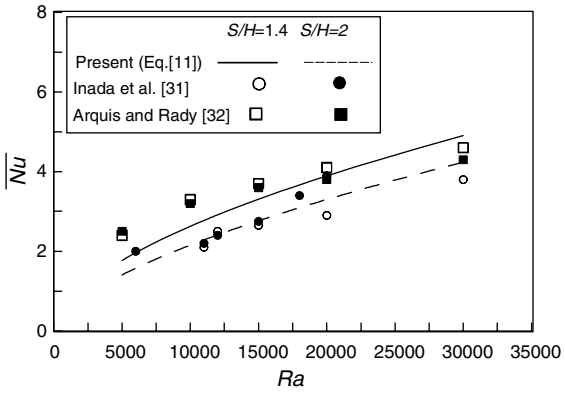

Fig. 10. Comparison with previous work.

flows, which in general tend to be unstable, the heat transfer and flow behaviors are sensitive to 3-D effects, especially in case of horizontal cavities heated from below.

7. Fin effectiveness

Heat transfer enhancement in enclosures due to using fins is measured by finned surface effectiveness (ε). It is defined as the ratio of the total heat transfer rate in presence of fins to that in absence of fins:

$$\varepsilon = \frac{Nu_{\mathrm{H}}}{Nu_{\mathrm{H\ no\ fins}}} \tag{13}$$

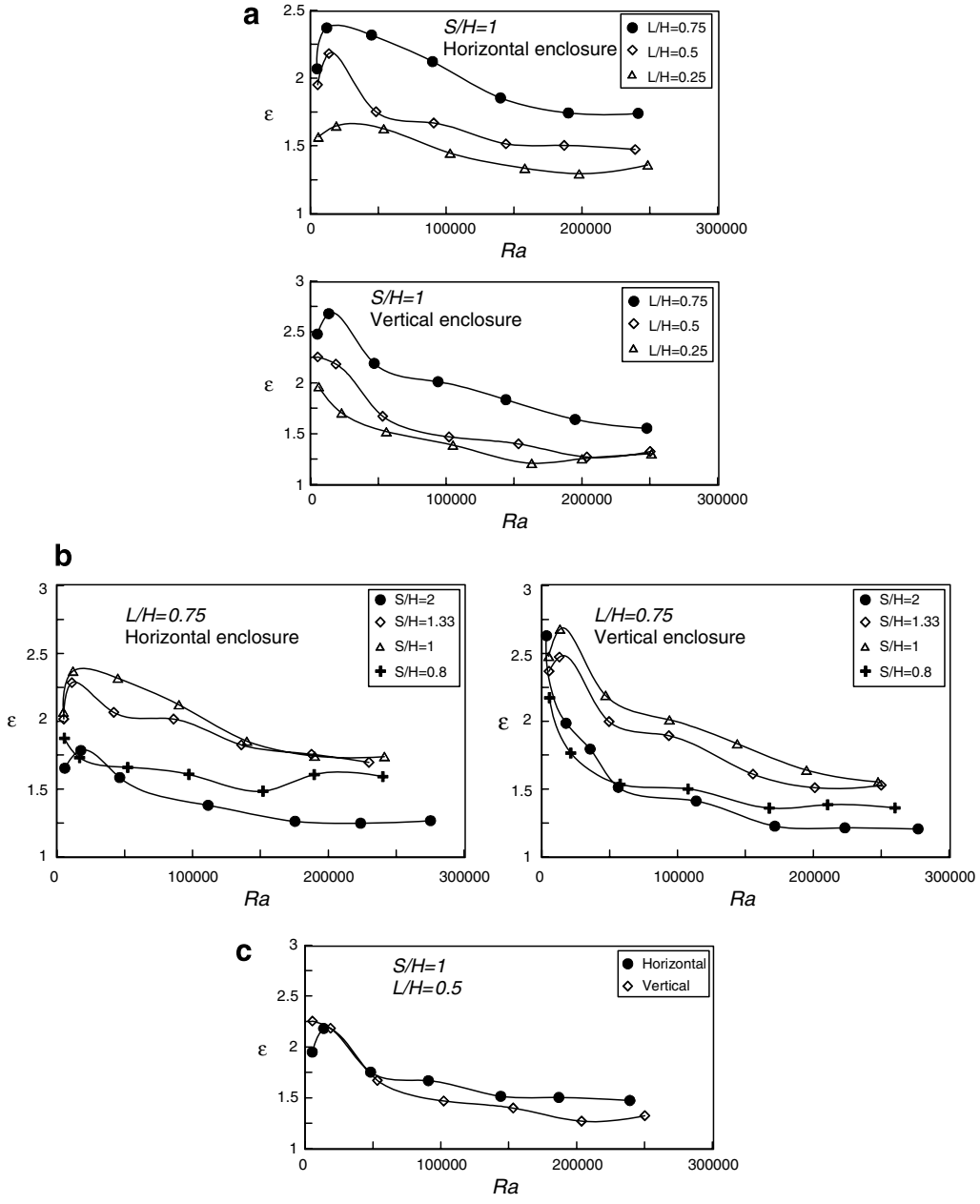

Fig. 11. Effect of fin length, fin spacing and enclosure orientation on fin effectiveness: (a) effect of fin length; (b) effect of fin spacing and (c) effect of enclosure orientation.

The finned surface effectiveness is an important parameter in design of finned surface. The aim of the designer is to choose the geometric parameters of the fin array that give maximum ε for a given Ra; i.e., for a given temperature difference $(T_H - T_L)$. The dependence of ε on S/H, L/H and the enclosure orientations are shown in Fig. 11 at a wide range of Ra. It should be noted that, to calculate ε using Eq. (13) at a certain Ra, the $Nu_{H\ no\ fins}$ is required at the same Ra. This was obtained from curve fitting of the data of the enclosure with a bare heated base plate (no fins) that are shown in Figs. 3 and 4. Fig. 11 shows that ε is always greater than one for any S/H and L/H, and through the entire range of Ra. Values of ε greater than one indicate enhancement of heat transfer due to using fins. For the present range of Ra, Fig. 11(a) shows that ε is a strong function of L/H for both horizontal and vertical enclosures; ε increases with increasing L/H. This is attributed to the increase of Nu_H with increasing L/H as discussed in Section 4.2. Also, Fig. 11 shows that the enhancement of ε due to increasing L/H decreases with increasing Ra. This can be attributed to the decrease of the rate of increase of Nu_H with L/H with increasing Ra. Fig. 11(b) shows the increase of ε with the decrease of S/H until it reaches a maximum at certain S/H, after which ε decreases with further decreasing of S/H. This can be attributed to the nature of variation of Nu_H with S/H as discussed in Section 4.1. A fin spacing of $S/H = 1$ seems to be an optimum value for maximum ε. Fig. 11(c) shows the effect of enclosure orientation on ε. As shown in the figure, at $Ra < 20{,}000$ the vertical enclosure has higher ε. However, at $Ra > 20{,}000$, the horizontal enclosure has higher ε.

Fig. 11 shows the decrease of ε with increasing Ra. This can be attributed to the rates of increase of Nu_H and $Nu_{H\ no\ fins}$ with Ra. As shown in Figs. 3–6, the rate of increase of $Nu_{H\ no\ fins}$ with Ra is higher than that of Nu_H. This can be attributed to the increase of the resistance to flow circulation with fin insertion. Careful examination of Fig. 11 reveals that at $Ra < 10{,}000$ and high S/H, ε increases with increasing Ra until it reaches a maximum after which ε decreases with further increasing of Ra. This may be due to the low flow circulation resistance at low Ra and high S/H.

8. Summary and conclusions

Experimental investigation of heat transfer and fluid flow characteristics in horizontal and vertical narrow closed enclosures having a heated finned base plate has been carried out. The effects of fin length and fin spacing have been studied for both orientations at a wide range of Rayleigh number. It has been found that insertion of fins with any fin array geometries increases the rate of heat transfer. Quantitative comparisons of heat transfer rate and surface effectiveness for both enclosure orientations have been reported. Optimization of fin-array geometries for maximum Nusselt number and finned surface effectiveness has been conducted. It was found that: (1) for a high range of Ra, increasing Ra increases Nusselt number and decreases fin effectiveness; (2) for a small range of Ra and at large S/H, increasing Ra increases both of Nusselt number and finned surface effectiveness; (3) Nusselt number and finned surface effectiveness increases with decreasing S/H until S/H reaches a certain value beyond which the Nusselt number and finned surface effectiveness start to decrease with further decreasing of S/H; (4) the maximum value of Nusselt number and finned surface effectiveness occurs at $S/H = 1$ for both enclosure orientations and (5) the Nusselt number and finned surface effectiveness increased with increasing fin length. Useful design guidelines and correlations were developed for both enclosure orientations. The predictions of these correlations were compared with the present and previous experimental data and good agreement was found.

References

[1] A. Bejan, Convection Heat Transfer, Wiley, New York, 1984.
[2] I. Catton, Natural convection in enclosures, Sixth Int. Heat Transfer Conf., Toronto 7, 1979, 13–43.
[3] A. Bejan, C.L. Tien, Laminar natural convection heat transfer in a horizontal cavity with different end temperatures, J. Heat Transfer 100 (1978) 641–647.
[4] S. Kimura, A. Bejan, The boundary layer natural convection regime in a rectangular cavity with uniform heat flux from the side, J. Heat Transfer 106 (1984) 98–103.
[5] D.A. Bratsun, A.V. Zyuzgin, G.F. Putin, Non-linear dynamics and pattern formation in a vertical fluid layer heated from the side, Int. J. Heat Fluid Flow 24 (2003) 835–852.
[6] M.W. Nansteel, R. Gerif, An investigation of natural convection in enclosure with two and three dimensional partitions, Int. J. Heat Mass Transfer 27 (1984) 561–571.
[7] R. Jetli, S. Acharya, E. Zimmerman, Influence of baffle location on natural convection in a partially divided enclosure, Numer. Heat Transfer 10 (1986) 521–536.
[8] J. Neymark, C.R. Boardman, A.T. Kirkpatrick, R. Anderson, High Rayleigh number natural convection in partially divided air and water filled enclosures, Int. J. Heat Mass Transfer 32 (1989) 1671–1679.
[9] A. Bejan, Heat Transfer, Wiley, New York, 1993.
[10] G.D. Raithby, K.G.T. Holland, Nat. convection, in: W.M. Rosenhow, J.P. Hartnett, E.N. Ganic (Eds.), Handbook of Heat Transfer Fundamentals, second ed., McGraw-Hill, New York, 1985 (Chapter 6).
[11] C.K. Choi, J.H. Park, M.C. Kim, J.D. Lee, The onset of convective instability in a horizontal fluid layer subjected to a constant heat flux from below, Int. J. Heat Mass Transfer 47 (2004) 4377–4384.
[12] M.C. Kim, L.H. Kim, C.K. Choi, The onset of convective motion in a horizontal fluid layer heated from below and cooled from above with constant heat flux, Int. Commun. Heat Mass Transfer 31 (2004) 837–846.
[13] M.T. Hyun, M.C. Kim, Onset of buoyancy-driven convection in the horizontal fluid layer subjected to time-dependent heating from below, Int. Commun. Heat Mass Transfer 30 (2003) 965–974.
[14] D. Mukutmoni, K.T. Yang, Rayleigh–Bénard convection in a small aspect ratio enclosure, Part I: Bifurcation to oscillatory convection, J. Heat Transfer 115 (1993) 360–366.
[15] D. Mukutmoni, K.T. Yang, Rayleigh–Bénard convection in a small aspect ratio enclosure, Part II: Bifurcation to chaos, J. Heat Transfer 115 (1993) 367–376.

[16] D. Mukutmoni, K.T. Yang, Thermal convection in a small enclosure: A typical bifurcation sequence, Int. J. Heat Mass Transfer 38 (1995) 113–126.
[17] F.H. Busse, Non-linear properties of thermal convection, Rep. Prog. Phys. 41 (1978) 1929–1967.
[18] K.T. Yang, Transition and bifurcations in laminar buoyant flows in confined enclosures, J. Heat Transfer 110 (1988) 1191–1204.
[19] A.Y. Gelfgat, Different modes of Rayleigh–Bénard instability in two and three dimensional rectangular enclosures, J. Comput. Phys. 156 (1999) 300–324.
[20] K.E. Starner, H.N. McManus, An experimental investigation of free convection heat transfer from rectangular fin-arrays, J. Heat Transfer (1963) 273–278.
[21] J.R. Welling, C.B. Wooldridge, Free convection heat transfer coefficient from rectangular vertical fins, J. Heat Transfer (1965) 439–444.
[22] C.D. Jones, L.F. Smith, Optimum arrangement of rectangular fins on horizontal surfaces for free convection heat transfer, J. Heat Transfer (1970) 6–10.
[23] F. Harahap, H.N. McManus, Natural convection heat transfer from horizontal rectangular fin arrays, J. Heat Transfer (1967) 32–38.
[24] A. Bar-Cohen, Fin thickness for an optimized natural convection array of rectangular fins, J. Heat Transfer (1979) 564–566.
[25] E.M. Sparrow, C. Prakash, Enhancement of natural convection heat transfer by a staggered array of discrete vertical plates, J. Heat Transfer (1980) 215–220.
[26] R.V. Rammohan, S.P. Venkateshan, Experimental study of free convection and radiation in horizontal fin array, Int. J. Heat Mass Transfer 39 (1996) 779–789.
[27] H. Yüncü, G. Anbar, An experimental investigation on performance of rectangular fins on a horizontal base in free convection heat transfer, Heat Mass Transfer 33 (1998) 507–514.
[28] A. Güvenc, H. Yüncü, An experimental investigation on performance of rectangular fins on a vertical base in free convection heat transfer, Heat Mass Transfer 37 (2001) 409–416.
[29] A.L. Vollaro, S. Grignaffini, F. Gugliermetti, Optimum design of vertical rectangular fin arrays, Int. J. Therm. Sci. 38 (1999) 525–529.
[30] S. Baskaya, M. Sivrioglu, M. Ozek, Parametric study of natural convection heat transfer from horizontal rectangular fin arrays, Int. J. Therm. Sci. 39 (2000) 796–805.
[31] S. Inada, T. Taguchi, W.J. Yang, Effects of vertical fins on local heat transfer performance in a horizontal fluid layer, Int. J. Heat Mass Transfer 42 (1999) 2897–2903.
[32] E. Arquis, M. Rady, Study of natural convection heat transfer in a finned horizontal fluid layer, Int. J. Therm. Sci. 44 (2005) 43–52.
[33] F.P. Incropera, D.P. DeWitt, Introduction to Heat Transfer, Wiley, New York, 1995.
[34] N.V. Suryanarayana, Engineering Heat Transfer, West Publishing Company, New York, 1995.
[35] J.P. Holman, W.J. Gajda, Experimental Method for Engineers, McGraw Hill, New York, 1989.